Contrib. Mineral. Petrol. 68, 207–219 (1979)

Contributions to Mineralogy and Petrology

On the Origin of Andesite in the Northern Mariana Island Arc: Implications From Agrigan

Robert James Stern
Geological Research Division, Scripps Institution of Oceanography, La Jolla, California 92093, USA

Abstract. Magmatic evolution on the active volcano of Agrigan in the northern Mariana Island Arc is interpreted as resulting in the production of calc-alkaline andesites by the fractional crystallization of high-alumina basalt. Basaltic products predominate, but the ratio of andesites to basalts increases with time up to an event of voluminous andesitic pyroclastic ejection accompanied by caldera-collapse; post-collapse lavas are entirely basaltic. Moderate iron-enrichment is demonstrated for the volcanic suite, with indications of a progressive, pre-caldera decrease in iron-enrichment; post-caldera lavas display a return to moderate Fe-enrichment. Overall, the lavas are enriched in the LIL elements (K, Rb, Ba, Sr) and depleted in Ti, Mg, Cr, and Ni. From the oldest to the youngest pre-caldera volcanic sequence, the LIL elements increase 3–6X while Ca and Mg decrease by 50% or more. Approximately constant K/Rb (430 ± 60) and $^{87}Sr/^{86}Sr$ (0.7032–0.7034) indicate consanguinity of the basalts and the andesites. Cumulate plutonic xenoliths, common in the lavas, are composed of mineral phases also encountered as phenocrysts. The following order of crystallization is indicated: olivine; anorthite-bytownite; clinopyroxene; orthopyroxene and titanomagnetite. Co-existing xenolithic olivines (Fo_{74-83}) and plagioclase (An_{88-96}) are typical of calc-alkaline island-arc assemblages and contrast with assemblages in the tholeiites from the Mariana Trough to the west. The relatively fayalitic composition and low abundances of Ni in olivines and Cr in clinopyroxenes indicate equilibrium with an already-fractionated liquid. These data, along with structural evidence, high Ca in the olivines, and comparison of the observed assemblages with experimental studies, suggests that these xenoliths formed as crystal cumulates at the floor of a shallow (≤ 7 km) crustal magma chamber.

Major element modeling studies using the separation of observed xenocrystic and phenocrystic phases from assumed parental liquids reproduce the observed temporal and geochemical variations in the lavas. Trace element modeling parallels this evolution with the exception of Cr and Ni in the andesites. An extensive (16.3 km^3) gabbroic body is required by this modeling to be present beneath Agrigan to produce the inferred volumes of the various lithologies preserved in the volcano's evolution. The sum of stratigraphic, geochemical, and isotopic evidence on Agrigan supports the derivation of calc-alkaline andesite by the removal of about 75% solids from a high-alumina basalt accompanied by a process of K and Rb enrichment, such as volatile-transfer. Considerations of $^{87}Sr/^{86}Sr$, $^{143}Nd/^{144}Nd$, and $^{3}He/^{4}He$ isotopic data indicate that the source region of these parental liquids lies in the mantle, not subducted crust. In the northern Marianas, the model of a shallow-crustal origin for andesite is preferred over one requiring andesite generation in the deeper mantle and/or subducted slab.

Introduction

The evolution of island-arc volcanoes and calc-alkaline magmas is a problem considered fundamental to the understanding of orogenic development and continental growth. Over the past 10 years, the genesis of calc-alkaline (and especially andesitic) magmas has been ascribed to processes operating in the mantle, either by fractional fusion of subducted oceanic lithosphere (Green and Ringwood, 1968; Fitton, 1971; Marsh and Carmichael, 1974) or in the superjacent mantle wedge (Kushiro, 1972; Arculus and Curran, 1972). However, there is also a growing body of data supporting earlier ideas which favored a crustal origin for andesites, either by anatexis of older sial or eugeosynclinal accumulations, or by fractional crystalliza-

0010-7999/79/0068/0207/$02.60

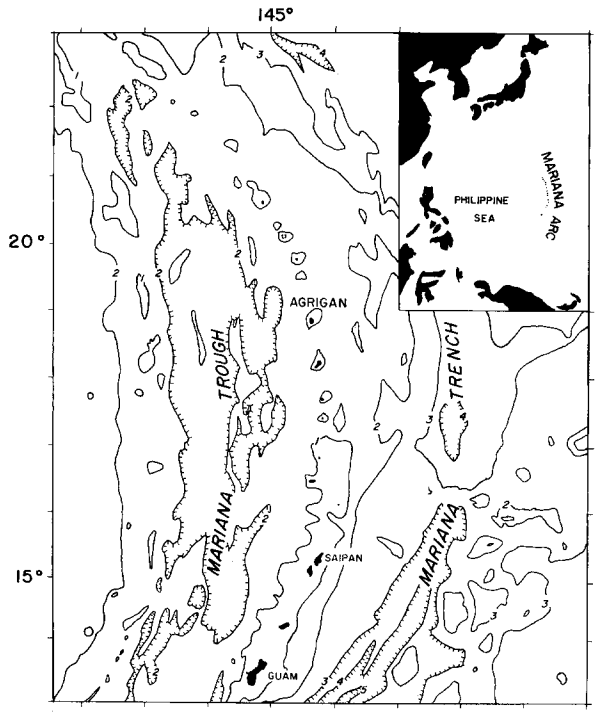

Fig. 1. Tectonic setting of Agrigan in the Mariana Island Arc. Bathymetric contours are in thousands of fathoms

tion of basalt (Kuno, 1968; Ewart and Bryan, 1973; DePaolo and Wasserburg, 1977). Processes of assimilation and anatexis of pre-existing crustal materials at continental or protocontinental convergent margins would contribute a lowest-melting fraction enriched in SiO_2, K, Na, Rb, Sr, Ba, $^{87}Sr/^{86}Sr$, etc., to more primitive liquids generated at greater depth. Such a process would produce andesites that nonetheless are not characteristic of liquids generated in the mantle. Magmatic evolution at convergent margins where evolved crust already exists (e.g., Andes, Cascades, Indonesia, Central America) is thus not considered diagnostic of processes responsible for the evolution of the calc-alkaline suite at ensimatic or intra-oceanic convergent margins. The situation of the latter type of volcanic arcs largely precludes the contamination of mantle-derived liquids by sial or thick sedimentary piles. Thus, the study of magmatic evolution on the ensimatic arcs is considered critical to our understanding of magmas generated above the Benioff Zone and the non-anatectic origin of andesite. The truly intra-oceanic island arcs are restricted to the circum-Pacific. These include the western Aleutians, central Kuriles, South Sandwich Islands, Tonga-Kermadec system, and the discontinuous chain of volcanoes extending from the Izu Peninsula, Japan, south through the Volcano Islands to the northern Mariana archipelago. It is the volcanic island of Agrigan[1], found in the southern part of the northern Mariana arc, that is the focus of this study (Fig. 1).

The purpose of this paper is to present and consider evidence for extensive, shallow-crustal fractionation beneath Agrigan and to discuss the likelihood of generation of Agrigan's andesites from its basalts by such processes. This is approached by outlining the stratigraphic variations in the geochemistry of the lavas, the constraints inferred from Sr-isotopic data, and evidences from plutonic ejecta. These data provide the basis for the development of a magmatic evolutionary model.

Stratigraphic Geochemical Trends

Five episodes of volcanism are identified on Agrigan. These are, from oldest to youngest: Old Volcanics, Pre-Caldera Volcanics, Breccia-Dike Complexes, Mantling Tuffs, and New Eruptive Centers (Stern, 1978). The first three predate caldera-collapse and contemporaneous eruption of andesitic pyroclastic ejecta; post-collapse magmatic resurgence has been basaltic. Figure 2 demonstrates the geochemical variation analyzed in these lavas. Although olivine is generally present in the mode, all lavas are quartz normative. An alkali-lime index of 59 identifies the series as calc-alkaline (Peacock, 1931); on an alkalies vs. silica diagram, the analyses plot in the high-alumina field (Kuno, 1966). Mild iron-enrichment of the succession demonstrates its tholeiitic affinities (Fig. 3; Irvine and Barragar, 1971; Miyashiro, 1974). The basalts have abundances of U (0.34–0.39 ppm), K_2O (0.37–1.01%), Rb (8–21 ppm), Sr (283–378 ppm), Ba (86–196 ppm), and K/Rb (370–490) which are similar to values suggested to be characteristic of the calc-alkaline suite (Jakes and White, 1972). Igneous products of other northern Mariana volcanoes are chemically similar to those of Agrigan (Schmidt, 1957; Meijer, 1974). In this respect, the evolution of Agrigan may be typical of magmatic development throughout this island arc. The entire arc should be considered as calc-alkaline, with LIL enrichments becoming extreme along its northern extension, culminating in the trachyandesites of Iwo Jima (29,600 ppm K, 1,078 ppm Ba, 69.6 ppm Rb, K/Rb=425; Philpotts et al., 1971).

Except along the coast and in the walls of the as-yet unexplored central caldera, good exposures of fresh rock are limited. Steep overgrown slopes restrict access to all but outcrops in coastal promontories and cliffs, and most of the samples analyzed for this study were collected here. This results in an inherent bias in the data presented herein. Nevertheless, the composition and proportions of lavas exposed along the coast should not differ greatly from other, unexposed portions of the subaerial volcano. For this reason, it is believed that the geochemical characteristics of the analyzed sample population is a good approximation to the petrologic composition and proportions of subaerial Agrigan lavas. Using the criteria that basalt $<53\%$ SiO_2, $53\% \leqq$ basaltic andesite $<55\%$ SiO_2 and andesite $\geqq 55\%$ SiO_2, 60% of the analyzed flows are basalts, 23% are basaltic andesites, and 17% are andesites. From the oldest to the youngest of the pre-caldera succession, the proportion of basalt:basaltic andesite:andesite becomes pro-

[1] Outlines of the structural setting of the N. Marianas (Hess, 1948; Karig, 1971), and discussion of previous studies of Agrigan, as well as discussions of its structure, stratigraphy, and petrography can be found elsewhere (Stern, 1978)

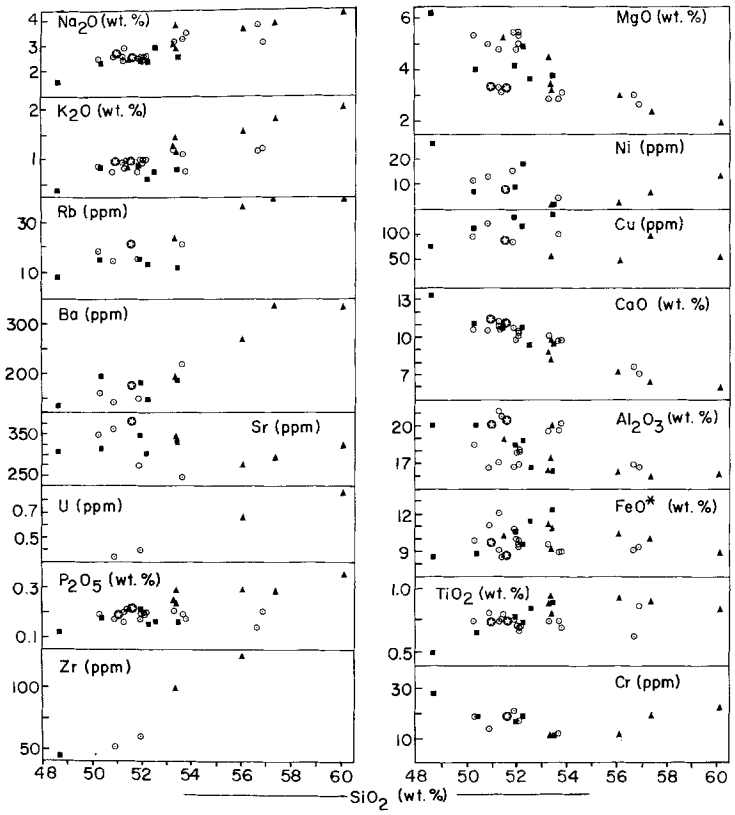

Fig. 2. Major and selected trace element variation diagrams. Symbols represent analyzed lavas from identified stratigraphic units. These are, from oldest to youngest: ■ = Old Volcanics; ○ = Pre-Caldera Volcanics; ▲ = Breccia-Dike Complexes; * = New Eruptive centers. Analytic methods and error discussed in Appendix I. Tabulated analytic data available from the author upon request

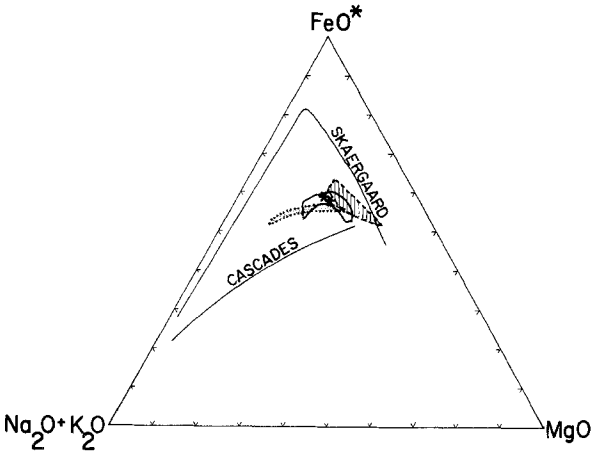

Fig. 3. AFM diagram for analyzed lavas of Agrigan. Dashed line enclosing field with vertical horizontal lines represents analyzed lavas from the Old Valcanics. Solid line enclosing blank field represents samples of the Pre-Caldera Volcanics. Dotted line enclosing stippled pattern represents the Breccia-Dike Complexes. Stars represent two analyzed lavas of the New Eruptive Centers

gressively weighted toward the felsic end, varying from 82:18:0 to 72:20:13 to 14:43:43. Andesitic pyroclastics associated with caldera-collapse have not been analyzed but appear in the field to be composed of andesite and dacite. Lavas erupted after the culmination of caldera-collapse are entirely basaltic.

The progressive enrichment in silica found in the pre-caldera volcanic succession is accompanied by a slight decrease in iron-enrichment. The "F" component shown on an AFM diagram decreases from a minimum of 63% in the Old Volcanics to 59% in the Pre-Caldera Volcanics to 57% in the Breccia-Dike Complexes; lavas erupted subsequent to caldera-collapse resume a moderate Fe-enrichment trend (Fig. 3).

Other elements reflect an overall temporal progression from mafic to more felsic that also was terminated by caldera-collapse (Fig. 2). The incompatible alkali metals and alkaline earths show especially profound variations from the older to younger pre-caldera volcanic episodes: (K_2O: 0.37–2.06%; Na_2O: 1.57–4.25%; Rb: 8–40 ppm; Ba: 86–336 ppm). The highly charged, incompatible elements also reflect this temporal progression in composition: (P_2O_5: 0.12–0.35%; U: 0.34–0.80 ppm; Zr: 45–125 pp,). Conversely, the ferromagnesium and related elements vary antipathetically with time (and silica), especially MgO (6.19–2.11%) and CaO (13.32–5.81%). Total iron as FeO*, Cu, and TiO_2 show moderate enrichments throughout the early part of the range, but later decrease in concentration. Abundances of Cr and Ni are always low (< 30 ppm), but generally decrease over the earlier parts of the range before returning to higher concentrations (10–20 ppm) in the younger lavas. Al_2O_3 and Sr show no progressive variation, with concentrations around $18.5 \pm 2.5\%$ and 310 ± 65 ppm respectively. Mean elemental ratios, indicative of fractionation, also relate the overall progression from the oldest to the youngest precaldera lavas ($FeO^*/MgO = 2.36$–3.20; $K_2O/Na_2O = 0.29$–0.41; $CaO/Al_2O_3 = 0.58$–0.47).

If the analyzed lithologic proportions approximate subaerial volume relationships of Agrigan lavas, and if the elemental concentrations and ratios just discussed are representative of this part of its magmatic evolution, then several conclusions can readily be drawn:

(1) A model of fractional crystallization is preferred over a model of fractional fusion for the generation of the observed compositional range. The stratigraphic trend is significant: the oldest

magmatic products are least fractionated while those erupted just prior to caldera-collapse are markedly more fractionated. While a significant amount of compositional overlap exists between the rocks of these three units, as a rule, the older lavas are enriched in the more refractory elements (Mg, Ni, Cr, Ca) and depleted in the magmaphile elements (Na, K, Rb, Ba, U, Zr, P) relative to the younger lavas. Clearly, a single event of fractionation of basalt to andesite is precluded by this compositional overlap. Nonetheless, considered overall, the observed temporal geochemical variations are consistent with a model of fractional crystallization of a basaltic parent, taking place in a magmatic reservoir where episodic replenishment is less than magma lost by eruption. On the other hand, fractional fusion of a unit volume of mantle peridotite would be expected to produce magmas showing a temporal variation opposite to that observed: LIL elements should be concentrated in the first melting fraction. Subsequent melts derived from this source would be progressively depleted in the LIL elements and enriched in more refractory elements producing a trend opposite to that observed. Variations involving the concept of partial fusion, such as zone-refining (Harris, 1957) also must be rejected for the same reason. Fractional fusion of subducted oceanic lithosphere would not be expected to result in any significant compositional variation in derivative liquids. A complex fractional fusion model, involving the fractionation of progressively smaller volumes of magma from independent sources in the mantle and/or subducted lithosphere, could be invoked. This model is not favored because it implies that the observed geochemical and temporal evolutionary patterns are coincidental and it is unlikely that such a process is responsible for the observed chemical consanguinity of the lavas.

(2) The culmination of magmatic evolution by the event of caldera-collapse favors a fractional crystallization model. This event of collapse is considered to have been caused by the withdrawal of support from the central portions of the edifice (Stern, 1978). This was effected by the violent expulsion of volatile-rich andesitic magma from a shallow magmatic reservoir. After collapse, resurgent magmatism resulted in the eruption of relatively unfractionated basalt. Thus, magmatic evolution was terminated by structural events which could only have affected the shallowest portion of the sub-volcanic magmatic system. The interpretation most consistent with these observations is that collapse of the edifice infilled part of a shallow, subjacent magma chamber. Diminution of the volume of the reservoir precluded continued fractionation, manifested by subsequent eruption of less-fractionated basalt. A model of fractional fusion for the generation of the compositional range does not explain this sequence of events.

(3) Consideration of inferred relative volumes of basalt, basaltic andesite, and andesite on Agrigan favors a fractional crystallization model. Objections to such a mechanism in the past have often focussed on the dearth of basalt in calc-alkaline volcanic provinces (Green and Ringwood, 1968). These objections cannot be applied to the magmatic evolution of Agrigan.

Sr Isotopes

$^{87}Sr/^{86}Sr$ is an excellent tool for considering consanguinity of magmatic products. A few analyses have been performed on Agrigan basalts in the past (Pushkar, 1968; DePaulo and Wasserburg, 1977). These are recorded along with two new analyses (Table 1).

$^{87}Sr/^{86}Sr$ determined in three different laboratories show a restricted range (0.70317–0.70344). The relatively non-radiogenic character of these lavas has been interpreted as consistent with an upper mantle origin for these lavas (Pushkar, 1968). While the $^{87}Sr/^{86}Sr$ of Agrigan is slightly more radiogenic than that of the abyssal tholeiites of the Mariana Trough (0.7026–0.7029; Hart et al., 1072; Meijer, 1976), they are similar to unequivocally mantle-derived, fresh tholeiites of the Indian Ocean floor (0.7032–0.7045; Subbarao and Hedge, 1973) and oceanic islands of the Pacific (0.7024–0.7056; Hedge, 1978). It is noteworthy that the Rb/Sr of the least fractionated Agrigan lava (9–1A; Rb/Sr = 0.026) is just adequate to generate the observed $^{87}Sr/^{86}Sr$ signature (0.7033 ± 00014) over the 4.6×10^9 years of earth history, using an assumed initial of 0.6998.

The relative invariance of $^{87}Sr/^{86}Sr$ with respect to increasing Rb/Sr is also significant. While Rb/Sr of 14 analyzed samples varies from 0.026 to 0.136, $^{87}Sr/^{86}Sr$ varies by 0.04%. Clearly, the high Rb/Sr of the andesites cannot have been thus maintained for very long. Assuming the Rb/Sr and $^{87}Sr/^{86}Sr$ of andesite 8–4 was evolved solely from the fractionation of a basaltic parent (9–1A), the more evolved magma could have possessed its present Rb/Sr for only about 50 million years. Furthermore, while the andesites are slightly more radiogenic than the basalts, the significance of this difference is not understood. Variations greater than the analytical error are found only for 8–4. The difference may be due to the role of a slightly less depleted portion of the mantle, a small slab component, or slight contamination by seawater. Resolution of the significance of this small difference requires additional determinations at a single laboratory. Nonetheless, it seems reasonable to infer that

Table 1. Rb/Sr and $^{87}Sr/^{86}Sr$ data for Agrigan

Sample	Lithology	Rb/Sr	$^{87}Sr/^{86}Sr$	Source
AG–4	Basalt	–	0.7032 ± 0.0010	Pushkar, 1968
1–3	Basalt	0.034	0.70319 ± 0.00006	DePaolo and Wasserburg, 1977
10–1	Basalt	0.053	0.70317 ± 0.00003	DePaolo and Wasserburg, 1977
7–1	Andesite	0.124	0.70335 ± 0.0002	This study
8–4	Andesite	0.136	0.70344 ± 0.0002	This study

the basalts and andesites are essentially isotopically consanguinous. It is concluded that their isotopic similarities permit the generation of the latter from the former.

Plutonic Xenoliths

A. Cumulate Nature of the Xenoliths

Compelling evidence of crystal fractionation is demonstrated by the common occurrence of cognate xenoliths. These are preserved in the lavas and tuffs of Agrigan, and are especially common in the Pre-Caldera Volcanics. Comprising up to 15% of an outcrop, they range in size from microscopic aggregates of a few crystals up to blocks 15 cm in diameter which display clear phase layering (Fig. 4). Although a few small clots consisting only of olivine and pyroxene are found, most of the inclusions are dominated by plagioclase. Nearly all of the xenoliths contain more than 50% plagioclase.

The inclusions can be subdivided on a basis of mineralogy. The following lists these types according to the phases present, with minerals listed in order of increasing abundance: (1) olivine-anorthite (allivalite); (2) clinopyroxene-olivine-plagioclase (troctolite and eucrite); (3) plagioclase (anorthosite); (4) clinopyroxene-plagioclase (gabbro and anorthositic gabbro); (5) titanomagnetite-orthopyroxene-clinopyroxene-plagioclase (gabbro and norite); (6) olivine-clinopyroxene (lherzolite). Table 2 lists the modes of a few of these xenoliths.

Modes of specimens which display as much phase layering and small-scale heterogeneity as these must be interpreted carefully. Nonetheless, the modes listed are representative of the overall mineralogy of the xenoliths as encountered in outcrop: plagioclase dominates over the mafics in most of the inclusions. Intercrystalline glass and vesicles occupy a relatively large volume in some xenoliths, causing these to be extremely friable. On the basis of field and laboratory petrographic observations, the "average Agrigan xenolith" consists of about 70–80% plagioclase and subequal proportions of olivine and augite with variable amount of glass and quench products.

The phase assemblage of the xenoliths is restricted to the 5 minerals observed as phenocrysts in the lavas: calcic plagioclase, olivine, pyroxene, and titanomagnetite. The observed order of crystallization is: olivine; plagioclase; augite; orthopyroxene and titanomagnetite. Hydrous phases never occur as constituents of the xenoliths. This contrasts with plutonic ejecta containing common hydrous components associated with West Indian volcanoes (Baker, 1968; Lewis, 1973; Rea, 1974) and the Cyclades (Nicholls, 1971). The minerals are generally unzoned except for thin rims where the crystals contact the intercumulus glass. Such a lack of zoning has been interpreted elsewhere as indicating adcumulus growth on previously precipitated crystals deposited on the floor of a magma chamber (Wager, 1962; Lewis, 1973). The euhedral olivines and plagioclases are often partially enclosed by interstitial clinopyroxene, which is interpreted as a manifestation of heteradcumulate growth (Wager and Brown, 1967). In one sample (7–4C), olivines display a remarkable dendritic habit and are up to 7 mm long. These are not poikilitic, rather, plagioclase laths surround them and show that the olivine 'tree' grew first, after which a covering of plagioclase developed (Fig. 5). Identical olivine morphology has been observed in the Skaergaard and Rhum layered gabbroic intrusions (Wager and Brown, 1967). In these localities, the dendritic habit of the olivines has been interpreted as resulting from the upward growth of this mineral from the floor of a magma chamber into the overlying liquid. The

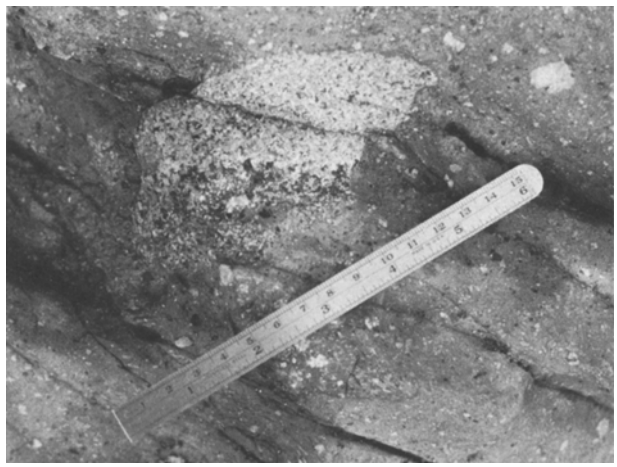

Fig. 4. Large cumulate xenolith encountered in Pre-Caldera Volcanics (4–4). Phase layering is evident: upper portion is anorthositic; lower portion is gabbroic. Notice partial disaggregation of gabbroic portion near 15 cm ruler

Table 2. Modes of some representative xenoliths

Xenolith	Plagioclase	Olivine	Clinopyroxene	Glass	Vesicles	Pts. Ctd.
5–2A	91.4%	4.2%	3.2%	1.1%	0.1%	1,000
4–4A	95.6%	0	0.4%	1.8%	2.2%	1,000
7–4C	54.6%	24.1%	1.2%	6.6%	13.5%	1,000
7–4D	69.6%	11.8%	0.5%	9.9%	8.2%	1,000

absence of vigorous current in the reservoir is required for the growth of these fragile crescumulates. Alternations of adcumulate and crescumulate textures in one sample (7–4C) suggest that episodes of magmatic quiescence alternated with periods of more vigorous currents.

The adcumulate, heteradcumulate, and crescumulate textures common in Agrigan xenoliths are believed to result from processes responsible for the development of similar textures in the large, well-studied stratiform bodies of Rhum and Skaergaard; specifically, these textures are the result of growth within or just above a crystal-liquid mush at the base or sides of a largely liquid magmatic reservoir. Larger-scale mineral banding is ascribed to gravitative settling of phases while crystal-liquid equilibrium underwent minor adjustment. The brown, vesicular glass found between crystals formed as the result of the sudden transport of nearly crystalline cumulate clusters from a hot environment at depth to the surface where the colder environment and vesiculation due to pressure loss resulted in the quenching of the intercrystalline residual liquid.

B. Xenolithic Mineral Chemistry

Analyses of various components of several of these xenoliths was undertaken using a combination of XRF and AA techniques on mineral separates and the electron microprobe as outlined in Appendix I. Chemical data are listed in Table 3; discussion of this data follows.

Plagioclase shows a restricted range of composition: An_{88-96}. Reverse or normal zoning is slight, with maximum variations of about 2% An. K_2O is very low ($\leq 0.08\%$).

Table 3. Analysis of mineral phases of Agrigan cumulate xenoliths. Except for samples labelled "mineral separate", analyses performed by electron microprobe. Mineral separates analyzed by combined XRF and AA techniques, outlined in Appendix I

	Olivine						Clinopyroxene		
	7–4D–1	7–4D–3		7–4C–1	7–4C–2	4–4A	7–4D–3	7–4C–3	
		Rim←	Core	Core	Core	Mineral Separate		Rim ←	Core
Na_2O							–	0.19	0.38
MgO	44.67	43.84	43.28	38.72	38.11	42.16	15.54	14.74	14.01
Al_2O_3	0.06	0.04	0.00	0.95	0.02	0.00	4.12	4.57	4.07
SiO_2	38.22	38.99	38.09	36.45	38.57	38.10	51.10	49.95	50.53
CaO	0.29	0.23	0.22	0.31	0.22	0.30	23.55	21.36	21.35
TiO_2	0.00	0.00	0.01	0.05	0.00	0.04	0.38	0.47	0.53
Cr_2O_3	0.06	0.00	0.00	0.01	0.00	0.01	0.04	0.00	0.11
MnO	0.28	0.28	0.32	0.42	0.38	0.28	0.08	0.15	0.16
FeO	16.33	17.05	18.09	23.10	23.20	17.69	6.55	7.59	8.01
NiO	–	0.03	0.05	0.08	0.00	–			
Total	100.11	100.46	100.06	100.09	100.50	98.59	101.36	99.02	99.15
Atoms to 4 oxygens							*Atoms to 6 oxygens*		
							Na	–	0.007	0.014
Mg	1.692	1.646	1.636	1.500	1.476	1.627	Mg	0.847	0.823	0.782
Al	0.001	0.001	0.000	0.029	0.000	0.000	Al^3	0.131	0.129	0.107
							Al^6	0.047	0.072	0.073
Si	0.971	0.982	0.966	0.974	1.002	0.987	Si	1.869	1.871	1.893
Ca	0.008	0.006	0.006	0.009	0.006	0.008	Ca	0.923	0.857	0.857
Ti	0.000	0.000	0.000	0.001	0.000	0.001	Ti	0.010	0.013	0.015
Cr	0.001	0.000	0.000	0.000	0.000	0.000	Cr	0.001	0.000	0.003
Mn	0.001	0.006	0.007	0.009	0.008	0.006	Mn	0.003	0.005	0.005
Fe	0.347	0.359	0.384	0.502	0.504	0.383	Fe	0.200	0.238	0.251
Ni	–	0.001	0.001	0.002	0.000	–				
$[Y]^6$	2.049	2.017	2.034	2.023	1.994	2.025	$[Y]^6$	2.031	2.016	2.000
Composition										
Fo	82.7	81.9	80.7	74.6	74.2	81	En	42.9	42.8	41.3
							Wo	46.8	44.6	45.2
							Fs	10.3	12.6	13.5

Table 3. (continued)

	Plagioclase									
	7–4D–1		7–4D–2	7–4D–3			7–4C–1	7–4C–2		4–4A Mineral Separate
	Rim ←	Core	Core	Rim ←	Inter-mediate ←	Core	Inter-mediate	Rim ←	Core	
Na_2O	0.69	0.61	0.51	0.48	0.66	0.72	1.29	1.11	1.19	0.43
MgO	0.04	0.04	0.00	0.07	0.06	0.03	0.10	0.08	0.11	0.05
Al_2O_3	35.74	34.91	35.54	35.59	35.34	35.85	33.82	32.98	33.07	35.3
SiO_2	44.64	44.16	44.65	43.98	43.95	44.32	45.96	45.79	45.56	43.7
K_2O	0.02	0.01	0.03	0.02	0.01	0.01	0.03	0.03	0.03	0.00
CaO	19.57	19.53	19.47	20.08	19.35	19.51	17.70	18.07	17.90	18.51
TiO_2	0.00	0.03	0.08	0.05	0.07	0.00	0.05	0.05	0.00	0.02
FeO	0.65	0.52	0.47	0.56	0.58	0.60	0.69	0.77	0.71	0.89
BaO	0.08	0.01	0.05	0.18	0.03	0.09	0.13	0.08	0.17	–
Total	101.43	99.82	100.80	101.01	100.05	101.13	99.77	98.96	98.74	99.37
Atoms to 8 oxygens										
Na	0.061	0.055	0.045	0.043	0.060	0.064	0.118	0.102	0.108	0.040
Mg	0.003	0.003	0.000	0.005	0.004	0.002	0.007	0.006	0.008	0.003
Al	1.929	1.919	1.928	1.940	1.934	1.940	1.880	1.857	1.828	1.948
Si	2.043	2.059	2.054	2.034	2.040	2.034	2.166	2.187	2.136	2.045
K	0.001	0.001	0.002	0.001	0.000	0.000	0.002	0.002	0.002	0.000
Ca	0.960	0.975	0.960	0.995	0.962	0.960	0.894	0.925	0.899	0.928
Ti	0.000	0.001	0.003	0.002	0.002	0.000	0.002	0.002	0.000	0.001
Fe	0.025	0.020	0.018	0.022	0.023	0.023	0.027	0.031	0.028	0.035
Ba	0.002	0.000	0.001	0.003	0.001	0.002	0.002	0.002	0.003	–
Z	3.972	3.978	3.982	3.974	3.974	3.974	4.046	4.044	3.964	3.993
X	1.052	1.055	1.029	1.071	1.052	1.051	1.052	1.070	1.048	1.007
Composition										
An	93.90	94.59	95.34	95.80	94.11	93.70	88.19	89.88	89.08	96.00
Ab	6.02	5.34	4.48	4.10	5.84	6.26	11.62	9.95	10.73	4.00
Or	0.09	0.08	0.18	0.10	0.04	0.05	0.19	0.16	0.20	0.00

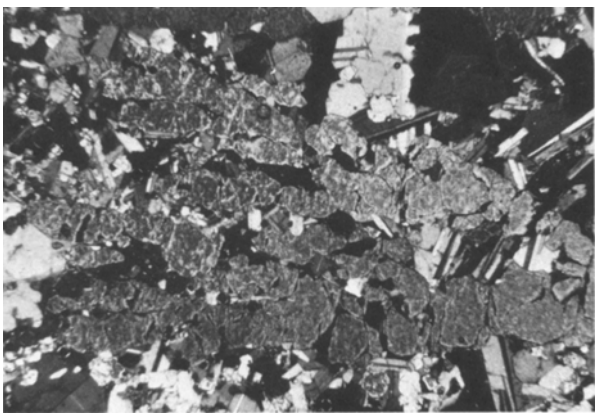

Fig. 5. Crescumulate olivine from xenolith in Pre-Caldera Volcanics (7–4C), under crossed nichols. Field of view is 6.5 × 4.3 mm

Forsterite contents of xenolithic olivines range from Fo_{74-83}. Reverse and normal zoning is also slight, less than 1.5% Fo; in conjunction with similar effects noted in plagioclases from the same xenolith (7–4D), this indicates that the reservoir was replenished by more primitive magma during the course of crystallization. NiO content of the olivines is low ($\leqq$0.08%). Olivines from basalt considered to be in equilibrium with a lherzolitic mantle (i.e., abyssal tholeiites and oceanic island basalts) have much higher concentrations of Ni in olivines of similar forsterite content (e.g., 2,000–2,200 ppm Ni at Fo_{90}; Simkin and Smith, 1970). This suggests that the xenolithic olivines did not crystallize from such primitive mantle melts, but were in equilibrium with an already-fractionated liquid. CaO is relatively high (0.22–0.31%), concentrations considered indicative of olivines crystallizing at low pressure (Simkin and Smith, 1970).

The co-existence of highly calcic plagioclase with relatively Fe-rich olivines is unknown from the tholeiitic layered intrusions of Rhum, Skaergaard, Stillwater, and the Bushveld. Typically, these bodies have plagioclase less calcic than An_{89}, which are associated with magnesian olivines (about Fo_{88}; Wager and Brown, 1967). Co-existing assemblages in the tholeiitic basalts of the Mariana Trough to the west are

Fo_{85-88} and An_{66-83} (Hart et al., 1972; Stern, unpublished data). The association of anorthitic plagioclase with relatively Fe-rich olivine such as observed on Agrigan is limited to plutonic ejecta from other island-arc volcanoes and calc-alkaline mafic and ultramafic layered intrusions (Lewis, 1973; Nishimori, 1976).

Intercumulus clinopyroxene is diopsidic augite, non-alkaline in character, with $Al_2O_3 = 4.07$–4.57, $Al^{IV}/Al^{IV} + Al^{VI} = 0.74$–$0.95$, $TiO_2 = 0.38$–0.53%, $Na_2O = 0.19$–0.38%, and $MnO = 0.08$–0.33%. Cr is low ($\leq 0.11\%$), another manifestation of crystal equilibrium with an already-fractionated liquid. Orthopyroxene is rare in the xenoliths, but is found along with titanomagnetite within inclusions associated with more fractionated lavas. Optical examination shows them to be hypersthene.

C. *Origin of the Xenoliths*

Stability of plagioclase is characteristic of low-pressure igneous environments, regardless of P_{H_2O} (Green and Ringwood, 1968; Yoder, 1969). P_{H_2O} in the parental magma is indicated to be moderate by considerations of the vesicular nature of lavas and frequent eruption of pyroclastics and by the common occurrence of large gas bubbles enclosed by glass in the xenoliths. Therefore, it does not seem unreasonable to suggest that $P_{H_2O} \approx P_{Total}$. Under these conditions, experimental studies on high-alumina basalts indicate that the phase assemblage and order of crystallization recorded in the xenoliths likely occurred at pressures of less than 2 kbars (Yoder and Tilley, 1962). Thus, the reservoir whose crystalline products of fractionation have been entrained in the lavas and whose inferred collapse produced the central caldera was probably located at a depth of no more than 7 km beneath Agrigan's summit. This supports the earlier conclusion, based on structural evidence, that Agrigan's crustal substructure includes a magmatic reservoir (Stern, 1978).

In spite of the modal abundance of plagioclase, the presence of cumulate olivines in the xenoliths precludes the role of plagioclase floatation in the generation of these cumulates. Crystal accumulation proceeded at the bottom and sides of the magma chamber. The xenoliths became incorporated in the lavas as the result of the disruption of basal cumulate layers and their subsequent entrainment in erupting magmatic liquids.

Discussion

The temporal magmatic evolution of Agrigan Volcano as represented by the deduced stratigraphic succession of analyzed lavas is most consistent with the development of younger, generally more fractionated liquids by a process of open-system crystal fractionation of a basaltic parent. The inferred overall volumes of basalt, basaltic andesite, and andesite as well as the temporal progression of their proportions supports such a model. Consanguinity is indicated by similarities in K/Rb and $^{87}Sr/^{86}Sr$. The nearly constant $^{87}Sr/^{86}Sr$ is considered especially significant in light of the observed 500% increase in Rb/Sr from most primitive to most fractionated liquids. The eruption of more fractionated liquids ended at the same time as an event of caldera collapse. This indicates that magmatic evolution transpired at depths that were shallow enough so that the collapse of the central portions of the edifice could upset the fractionating magmatic system. Finally, the ubiquitous presence of cognate xenoliths that are clearly of cumulate origin proves that crystal fractionation has played a significant role in magmatic evolution. Comparison of the mineralogy of these xenoliths with the results of experimental petrologic studies supports the interpretation that the fractional crystallization responsible for the formation of the xenoliths occurred in a crustal environment, at depths of 7 km or less.

Qualitatively, the evidence indicates that: (a) crystal fractionation has been an important aspect of the immediately sub-volcanic magmatic system of Agrigan, and; (b) the range of calc-alkaline eruptive products, from basalt to andesite, could be produced by such a process. This model was tested, using the computer-based petrologic mixing program of Wright and Doherty (1970). In this modeling, the most mafic sample of the oldest sequence was assumed to be parent material (9–1A). From this, the derivation of an aphyric basalt from the next youngest unit was modeled, which then served as the mother-liquid for the extraction of aphyric, younger basaltic-andesites and andesites. Major and selected trace element abundances of these five representative rocks are listed in Tables 4 and 5. Considering that the Fe^{III}/Fe^{II} of some of these samples may be partly the result of deuteric alteration non-diagnostic of magmatic fractionations, the Fe_2O_3 in some of these rocks was arbitrarily reset at 2.0%. Mineralogic composition used in the modeling were determined using the range of compositions analyzed from Agrigan xenoliths and phenocrysts. Plagioclase ranged in composition from $Ab_4An_{96}Or_{0.1}$ to $Ab_{30.4}An_{68.4}Or_{1.2}$. Olivine ranged from Fo_{54} to $Fo_{82.7}$. Clinopyroxene was assumed to be $En_{43.3}Wo_{42.5}Fs_{14.2}$. Titanomagnetite microphenocrysts were found to range in composition from $Usp_{9.9}$ to $Usp_{38.9}$. For the latest stages of fractionation, a solution permitting orthopyroxene was introduced; compositions ranging from En_{50-82} were allowed.

Table 4. Chemical composition and CIPW norms of Agrian lavas used in computer modeling of crystal fractionation. 9–1A is basalt from Old Volcanics, SSE coast. 1–3 is basalt from Pre-Caldera Volcanics, W. coast. 4–8 is basaltic andesite from Breccia Dike Complexes, S. coast. 8–4 is andesite from Breccia Dike Complexes, SSE coast. 7–1 is andesite from Breccia Dike Complexes, W. coast

	Chemical composition and CIPW norms of representative Agrigan lava				
	9–1A	1–3	4–8	8–4	7–1
SiO_2	48.7	50.9	53.3	57.4	60.1
TiO_2	0.49	0.80	0.88	0.88	0.81
Al_2O_3	20.0	16.6	16.3	15.9	16.0
Fe_2O_3	3.63	2.99	5.59	2.78	2.11
FeO	5.20	8.33	5.94	7.36	6.90
MnO	0.16	0.22	0.22	0.22	0.22
MgO	6.19	5.10	4.47	2.41	1.87
CaO	13.32	10.46	8.82	6.29	5.81
Na_2O	1.57	2.57	3.04	3.88	4.25
K_2O	0.37	0.73	1.20	1.80	2.06
H_2O^+	0.08,	0.13	–	0.42	0.29
H_2O^-	0.17	0.05	–	0.18	0.15
P_2O_5	0.12	0.17	0.25	0.28	0.35
Total	100.00	99.05	100.01	99.80	100.92
FeO*/MgO	1.37	2.16	2.45	4.09	4.71
K_2O/Na_2O	0.24	0.28	0.39	0.46	0.48
CaO/Al_2O_3	0.67	0.63	0.54	0.40	0.36
	CIPW norms, anhydrous, mol %				
	9–1A	1–3	4–8	8–4	7–1
Quartz	2.051	2.364	6.983	8.985	10.379
Feldspar					
Or	2.192	4.363	7.090	10.722	12.115
Ab	13.318	21.995	25.721	33.096	35.791
An	46.548	31.964	27.283	20.819	18.408
Diopside					
Wo	7.897	8.100	6.194	3.672	0.341
En	5.258	4.085	3.941	1.386	1.096
Fs	2.059	3.831	1.857	2.349	2.354
Hypersthene					
En	10.197	16.981	7.191	4.665	3.539
Fs	3.994	8.762	3.388	7.908	7.597
Mt	5.297	4.385	8.104	4.063	3.045
Il	0.933	1.537	1.671	1.685	1.531
Ap	0.285	0.407	0.592	0.669	0.825
	100.008	100.012	100.016	100.017	100.021

The results of this modeling are schematically presented in Fig. 6. This shows that the observed range in major element compositions can be evolved by extensive fractionation involving a reasonable parent and the observed range of xenolithic and phenocrystic mineral compositions. In this case, andesite 7–1 is the end product of the separation of more than 75% crystalline phases from basalt 9–1A, although some additional mechanism is required to explain the observed 550% enrichment in K_2O.

Table 5. Selected Trace Elements

	9–1A	1–3	4–8	8–4	7–1
Rb	8	14 (11.9)	23	40	39
Sr	305	342 (352)	342	294	314
Ba	86	142 (152)	192	336	333
Zr	45	51	99	–	–
U	–	0.34	–	–	0.86
Ni	26	13	1	6	13
Cr	28	14	11	19	22
Cu	75	121	56	90	26
K/Rb	380	430	420	370	440
Rb/Sr	0.026	0.041	0.067	0.136	0.124
K/Ba	36	43	50	44	51
Ba/Sr	0.28	0.42	0.56	1.14	1.06
K/U	–	1.8×10^4	–	–	2.0×10^4

Concentration in ppm. Analytical methods and errors outlined in Appendix I. Values in parentheses represent analyses of separate portion of the same hand specimen by D. DePaolo, CalTech

The computer-generated solution for major elements was tested by using the determined concentrations of selected trace elements for which crystal-liquid distribution coefficients can be estimated. In this test, the equilibrium expression for trace element variation during fractional crystallization was employed (Arth, 1976):

$$C_l = \frac{C_i}{F + D_s(1-F)} \quad (1)$$

where C_l, C_i refer to the concentrations of the trace element in the derivative and initial liquids, respectively, F refers to the fraction of liquid remaining at the completion of the process, and D_s is the bulk distribution coefficient given by:

$$D_s = \sum_{i=1}^{n} W^i K^{i/l} \quad (2)$$

where W^i is the proportion by weight of mineral "i" in the crystal separate and $K^{i/l}$ is its solid/liquid distribution coefficient for the pertinent element. As in the major element modelling, 9–1A is the assumed parent; using concentrations of trace elements determined for this sample and the values for F and W from the major element solution, trace element concentrations were predicted for 1–3, 4–8, 8–4, and 7–1. Values for distribution coefficients ($K^{i/l}$) are from various sources: Rb, Ba, and, Sr (Arth, 1976); Sr as a function of % An in plagioclase (Karringa and Noble, 1971); Cr and Ni (Davis and Condie, 1977). The results of these calculations are shown in Fig. 7; analyzed concentrations are listed for comparison.

The model predicts Rb values that are 10–35% lower than analyzed. This is similar to the general

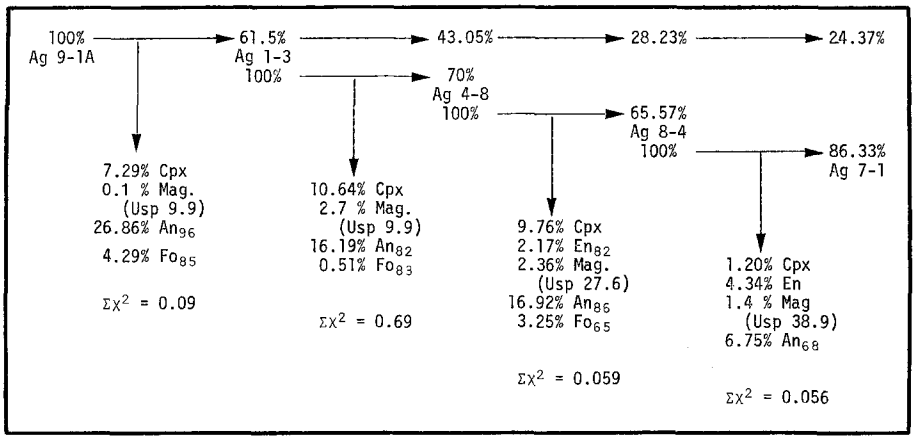

Fig. 6. Computer-modeled fractionation history of Agrigan magmatic system. Upper horizontal row of figures indicates percent of liquid remaining from the modeled crystal fractionation of assumed parent 9–1A. Lower row of figures represents percent of liquid remaining from the fractionation of the immediately preceeding liquid composition. Vertical columns represent compositions and amounts of computer-modeled removed solids as found to best mimic the observed compositional variations. $\sum X^2$ represents the sum of the squares of residuals between observed and modeled liquids

		9-1A → 1-3 F = 0.615			1-3 → 4-8 F = 0.700			4-8 → 8-4 F = 0.656			8-4 → 7-1 F = 0.863		
		D_s	Predicted	Observed	D_s	Predicted	Observed	D_s	Predicted	Observed	D_s	Predicted	Observed
Rb	8	0.055	13	14	0.049	18	23	0.046	27	40	0.045	31	39
Sr	305	0.846	324	342	1.121	313	342	0.871	326	294	1.249	315	284
Ba	86	0.163	127	142	0.133	172	192	0.122	246	336	0.136	279	333
Ni	26	2.76	16	13	2.31	11	1	3.33	6	6	3.19	5	13
Cr	28	2.98	9.4	14	10.29	3	11	8.37	1	19	9.0	1	22

Fig. 7. Trace-element testing of computer-generated major element fractionation history for Agrigan lavas. F (as defined in text) is determined from the major element solution. D_s is generated from W (from major element solution) and $K^{\alpha/L}$ (from various sources). Predicted values are those expected from the fractionation of crystalline phases indicated by the computer-generated major element solution. Determined concentration listed for comparison

underprediction of K_2O in the major-element solution and suggests that some mechanism exists for enriching the residual magma in K and Rb. Preferential entrainment and upward transfer of these elements in vapor phase (McKay et al., 1972; Bryan and Moore, 1977) is especially attractive in view of the observed increase of ratios of both K and Rb with other, less volatile, incompatible elements. For example, from 9–1A to 7–1, K/Ba increases from 36 to 44 and K_2O/P_2O_5 increases from 3.1 to 5.9. From 1–3 to 7–1 K/U increases from 1.8 to 2.0×10^4. K/Rb stays in the range 370–440, with no systematic variation along the compositional range. Volatile transfer of especially K and Rb is thus considered likely to make a contribution to elemental abundances in liquids situated in the upper portions of the Agrigan magma chamber.

Correspondence between modeled and observed Sr abundances is good, differing by about $\pm 10\%$. Noteworthy is the relative invariance of Sr concentrations, both modeled (315 ± 11 ppm) and observed (313 ± 29 ppm). This variation of less than 20% over the entire range of compositions indicates extensive control by calcic plagioclase ($K_{Sr}^{Pl/l} = 1.4$–2; Karringa and Noble, 1971) providing confirmation of the proposed model of plagioclase-rich crystal fractionation.

Agreement between modeled and observed Ni and Cr abundances is adequate in the range basalt to basaltic-andesite. However, discrepancies become large in the andesites, especially for Cr. This has been cited as indicating that andesite cannot be derived by the fractional crystallization of basalt (Taylor et al., 1969). On the other hand, when lavas are as depleted in these elements as the Agrigan lavas are, incorporation of very small amounts of a mineral that is rich in that element will greatly increase the analyzed concentration. The presence of xenocrysts has already been noted and the incorporation of mi-

Table 6. Average composition of Agrigan subvolcanic cumulate body

SiO_2	44.43%	Feldspar	Or	0.177
Al_2O_3	23.23		Ab	2.847
Fe_2O_3	1.02		An	59.981
FeO	5.51	Nepheline		1.850
MgO	7.71	Diopside	Wo	10.132
CaO	16.98		En	6.442
Na_2O	0.74		Fs	3.041
K_2O	0.03	Olivine	Fo	8.943
TiO_2	0.24		Fa	4.653
P_2O_5	0.00	Magnetite		1.479
MnO	0.10	Ilmenite		0.456
Total	99.99%			100.001

nute amounts of such material into the generally aphyric samples is likely. Other sources of error that might contribute to the deviation of modeled from analyzed trace element include (1) uncertainties in trace element distribution coefficients (Arth, 1976); (2) failure of equilibrium model to hold at very low trace element concentrations (Albarede and Bottinga, 1972); (3) analytical uncertainty.

Using the modeled major element solutions for the evolution of Agrigan lavas, the volume of crystalline residuum required to produce the lavas developed in the subaerial portion of the volcano may be estimated. Representing Agrigan as a perfect cone ($h=$ 1 km, $r=4$ km), the subaerial part of the volcano has a volume of 16.8 km^3. Assuming that the analyzed proportions of the lavas (60% basalt, 23% basaltic-andesite, and 17% andesite) represent the weight proportions of these lithologies in the subaerial portions of the volcano, then subaerial Agrigan is composed of 2.8×10^{13} kg basalt, 1.0×10^{13} kg basaltic-andesite, and 0.7×10^{13} kg andesite. Further assuming 9–1A as representative of a parental liquid, 1–3 as typical Agrigan basalt, 4–8 as typical Agrigan basaltic-andesite, and 7–1 as typical andesite, then 4.9×10^{13} kg of cumulate residuum is present beneath Agrigan. Assuming a gabbroic density of 3.0 g/cc, then this residuum represents a plutonic body occupying 16.3 km^3 beneath Agrigan. The calculated chemical and normative composition of this body is listed in Table 6. This is an olivine gabbro, comparable to the 'average Agrigan xenolith'.

The nature of the parental magma is an unresolved problem. Sample 9–1A has been assumed for this role, at least for the purpose of generating the younger and more fractionated lavas. Nonetheless, even this rock has FeO*/MgO > 1, low Cr and Ni (< 30 ppm), and is enriched in LIL elements relative to the supposed primitive magmas of intra-oceanic island arcs (Jakes and White, 1972). This evidence makes it likely that it, too, represents the product of some sort of fractionation process. A possible parental liquid to 9–1A might be similar in some respects to the aphyric tholeiites recovered from the Mariana Trough. The most representative of these contain 6.8% FeO*, 7.7% MgO, 0.2% K_2O, and 0.8% TiO_2 (Stern, unpublished data). Separation of 5–10% olivine and some Ti-bearing phase in tandem with some process such as vapor transfer for enriching derivative liquids in the LIL elements might be responsible for the generation of the most primitive of the subaerial volcanics on Agrigan. Conceivably, this aspect of magmatic evolution is recorded in the lavas of the submarine portion of Agrigan. Data on the form and composition of this part of the volcano are lacking, but assuming it rests on the Mariana Ridge at a depth of 3.5 km below sea-level (Stern, 1978) and further assuming the average subaerial slope (20°) is maintained throughout, then about 1,000 km^3, or 98% of the total volcanic volume, is submerged. If this part of the volcano represents fractionation of basalt similar to 9–1A from a tholeiitic parent, then a very considerable volume (50–100 km^3) of ultramafic crystal residue may exist beneath the layered gabbroic complex under Agrigan.

Whatever the chemical composition of the parental liquid may be, its source is an unresolved problem. Isotopic constraints seem to be most successfully employed in discussions of its nature. On the basis of combined Pb and Sr isotopic data, Meijer (1976) concluded that the source of recent Mariana arc magmas lay, in part, in altered and subducted Pacific Ocean crust. However, the samples from Anatahan and Pagan analyzed by Meijer are significantly more radiogenic ($^{87}Sr/^{86}Sr = 0.70374$–$0.70380$) than those from Agrigan (0.70317–0.70344). The significance of this inter-island variation is not understood, but assuming that the Agrigan lavas are similar in their $^{206}Pb/^{207}Pb$ to the samples analyzed by Meijer, they would plot well within the $^{206}Pb/^{207}Pb$ vs. $^{87}Sr/^{86}Sr$ field he has defined for lavas of the ocean basins. Furthermore, the defined island-arc field is completely overlapped by the field of oceanic island basalts. Evidence that the partial melting of altered and subducted oceanic crust has contributed to the isotopic signature of Mariana Island Arc magmas must be considered equivocal.

DePaolo and Wasserburg (1977) used another isotopic variation diagram in an attempt to resolve the problem. They plotted $^{143}Nd/^{144}Nd$ vs. $^{87}Sr/^{86}Sr$ for unequivocal mantle derivatives (alkali basalts of the oceanic islands, abyssal tholeiites) and for Agrigan lavas. Since the hydrothermal alteration of oceanic crust results in higher $^{87}Sr/^{86}Sr$ while $^{143}Nd/^{144}Nd$ should remain constant, they considered that the frac-

tional fusion of such material in the Benioff Zone should produce liquids significantly enriched in $^{87}Sr/^{86}Sr$ relative to $^{143}Nd/^{144}Nd$ when compared with "normal" mantle derivatives. Instead, the Agrigan lavas occupy a position on the $\varepsilon_{Sr}-\varepsilon_{Nd}$ correlation line as defined by abyssal tholeiites and oceanic island basalts. DePaolo and Wasserburg concluded that their data were most consistent with the derivation of the Agrigan lavas from a mantle reservoir which is isotopically intermediate between those responsible for the generation of abyssal tholeiites and oceanic island basalts.

Determination of $^{3}He/^{4}He$ on water samples from an Agrigan hot spring supports the interpretation of a mantle source for the basalts. These waters are enriched in ^{3}He, showing a $^{3}He/^{4}He$ that is seven-times that of the atmospheric ratio. This is lower than, but still comparable to, the 10-times-atmospheric ratio of abyssal tholeiitic glasses, leading Craig et al. (1978) to conclude that the flux of these volatiles was due to the degassing of the autochthonous, sub-volcanic mantle.

The body of data concerning the problem of the ultimate origin of Agrigan magmas in particular and island arc magmas in general is still growing. Further studies are urgently needed if the controversy is to be resolved, but the data collected on Agrigan to date seem most consistent with the derivation of the primitive liquids by the fractional fusion of mantle peridotite and not by the extensive participation of altered and subducted oceanic crust and sediments.

Conclusion

The bulk of geochemical, mineralogical, and isotopic evidence as deciphered by the analysis of Agrigan lavas supports an interpretation of a crustal origin for Agrigan andesites. The subordinate andesitic lavas of Agrigan are believed to derive from the fractional crystallization of a basaltic progenitor. While the exact composition of this parental liquid is unresolved, the petrologic charanceristics of derivative liquids share similarities both with abyssal tholeiites (low Ti, high Al, moderate Fe-enrichment) and with alkali basalts of oceanic islands (moderate to high K, Rb, Ba; moderate K/Rb and K/Ba). $^{87}Sr/^{86}Sr$ and $^{143}Nd/^{144}Nd$ data further indicate that the isotopic characteristics of the Agrigan source region(s) are intermediate between those of abyssal tholeiites and ocean island basalts. Combined with $^{3}He/^{4}He$, the data do not indicate the extensive participation of subducted crust during magmagenesis. Further studies are required if we are to fully resolve the question of the source region characteristics and parental liquid compositions of the Marianas and other island arc magmatic systems. Nonetheless, the results of this study indicate that the andesites of Agrigan are *not* derived deep in the mantle or subducted crust, but should be considered as consequences of the fractional crystallization of basalt.

Acknowledgements. This study benefitted from the assistance and encouragement of A.E.J. Engel, J.W. Hawkins, D. Macdougall, A. Meijer, and T. Dixon. Carl Hedge made possible the Sr isotope determinations at the U.S.G.S. facilities in Denver. J. Carlson kindly produced the U analyses and T.J. Chow produced the Ba analyses. Michiko Hitchcox patiently typed numerous revisions of the manuscript. I am very grateful to all. And, especially to Melissa.

Appendix I

Analytical Methods

SiO_2, TiO_2, Al_2O_3, CaO, K_2O, P_2O_5, and total iron as FeO* were determined using X-ray fluorescence techniques on fused glass pellets (Clague, 1974). Working curves were generated using 3 replicates of U.S.G.S. standards: AGV, GSP, G-2, W-1, BCR, and PCC. Errors quoted represent the maximum deviation of the quoted values (Flanigan, 1973) from those predicted from the least-squares-fit working curve or the variation in concentration determined on replicate unknowns, whichever was greater. XRF errors are quoted below, in absolute concentration: $SiO_2 \pm 0.75\%$, $TiO_2 \pm 0.03\%$, $Al_2O_3 \pm 0.50\%$, $CaO \pm 0.19\%$, $K_2O \pm 0.09\%$, $P_2O_5 \pm 0.02\%$, $FeO^* \pm 0.22\%$. FeO was determined by titration (Shapiro and Brannock, 1956). Concentrations of Na_2O, MgO, MnO, Cu, Cr and Rb were determined using atomic absorption techniques (Clague, 1974), employing the same set of U.S.G.S. standards. Errors, in absolute concentration, are: $Na_2O \pm 0.25\%$, $MgO \pm 0.10\%$, $MnO \pm 0.01\%$, $Cu \pm 5$ ppm, $Cr \pm 4$ ppm, $Rb \pm 5$ ppm. Sr was determined by method of additions. U was determined by induced fission track methods (Macdougall, 1972). Zr and Ni were determined by XRF on pressed pellets. Errors are: Ni ± 5 ppm, Zr ± 40 ppm. Ba was determined by isotope dilution (Chow et al., in press). H_2O^- was determined by weight loss of the sample after drying at 110° C overnight; H_2O^+ is the difference between this and the total water determined by the 'rapid rock' ignition tube method (Shapiro and Brannock, 1956).

Most mineral analyses were performed at the California Institute of Technology, using a MAC 5-SA3 electron microprobe interfaced with a PDP-8/L computer. Errors approach 1–2% of the reported value for oxides with abundances greater than 10%; at lower concentrations errors increase greatly.

$^{87}Sr/^{86}Sr$ analyses were performed on unspiked samples at facilities of the U.S. Geological Survey in Denver. Analytical methods are as outlined elsewhere (Divis, 1974).

References

Albarede, F., Bottinga, Y.: Kinetic disequilibrium in trace element partitioning between phenocrysts and host lava. Geochim. Cosmochim. Acta **86**, 141–156 (1972)

Arculus, R.J., Curran, E.B.: The genesis of the calc-alkaline rock suite. Earth Planet. Sci. Lett. **15**, 255–262 (1972)

Arth, J.G.: Behavior of trace elements during magmatic processes: A summary of theoretical models and their application. J. Res. U.S. Geol. Surv. **4**, 41–47 (1976)

Baker, P.E.: Petrology of Mt. Misery Volcano, St. Kitts, West Indies. Lithos **1**, 124–150 (1968)
Chow, T.J., Earl, J.L., Reed, J.H., Hansen, N., Orphan, V.: Barium content of Southern California coastal sediments. Environ. Sci. and Tech. (in press)
Clague, D.A.: The Hawaiian-Emperor Seamount Chain: Its origin, petrology, and implications for plate tectonics. Ph.D. thesis, Univ. Calif. San Diego, U.S.A. (1974)
Craig, H., Lupton, J.E., Horibe, Y.: A mantle helium component in Circum-Pacific volcanic gases: Hakone, the Marianas and Mt. Lassen. Adv. Earth Planet. Sci. **3**, 43–56 (1978)
Davis, P.A., Condie, K.C.: Trace element model studies of Nyanzian greenstone belt, western Kenya. Geochim. Cosmochim. Acta **41**, 271–277 (1977)
DePaolo, D.J., Wasserburg, G.J.: The sources of island arcs as indicated by Nd and Sr isotopic studies. Geophys. Res. Lett. **4**, 465–468 (1977)
Divis, A.F.: The geology and geochemistry of the Sierra Madre mountains, Wyoming – The evolution of a Precambrian continental margin. Ph.D. thesis, Univ. Calif. San Diego, U.S.A. (1974)
Ewart, A., Bryan, W.B.: Petrology and geochemistry of Tongan Islands. In: The Western Pacific (P.J. Coleman, ed.) pp. 503–522. Nedlands, Western Australia: University of Western Australia Press 1973
Fitton, J.G.: The generation of magmas in island arcs. Earth Planet. Sci. Lett. **11**, 63–67 (1971)
Flanigan, F.J.: 1972 values for international geochemical reference standards. Geochim. Cosmochim. Acta **37**, 1189–1200 (1973)
Green, T.H., Ringwood, A.E.: Genesis of the calc-alkaline igneous rock suite. Contrib. Mineral. Petrol. **18**, 105–162 (1971)
Harris, P.G.: Zone refining and the origin of potassic basalts. Geochim. Cosmochim. Acta **12**, 195–208 (1975)
Hart, S.R., Glassley, W.E., Karig, D.E.: Basalts and sea floor spreading behind the Mariana Island Arc: Earth Planet. Sci. Lett. **15**, 12–18 (1972)
Hedge, C.E.: Strontium isotopes in basalts from the Pacific Ocean Basin. Earth Planet. Sci. Lett. **38**, 88–94 (1978)
Hess, H.H.: Major structural features of the western North Pacific, an interpretation of H. O. 5845, bathymetric chart, Korea to New Guinea. Geol. Soc. Am. Bull. **59**, 417–466 (1948)
Irvine, T.N., Barragar, W.R.A.: A guide to the chemical classification of common volcanic rocks. Can. J. Earth Sci. **8**, 523–548 (1971)
Jakes, P., White, A.J.R.: Major and trace element abundances in volcanic rocks of orogenic areas. Geol. Soc. Am. Bull. **83**, 29–40 (1972)
Karig, D.E.: Structural history of the Mariana Island Arc system. Geol. Soc. Am. Bull. **82**, 323–344 (1971)
Karringa, M.K., Noble, D.C.: Sr and Ba distribution between natural feldspar and igneous melt. Earth Planet. Sci. Lett **11**, 147–151 (1971)
Kuno, H.: Lateral variation of basalt magma types across continental margins and island arcs. Bull. Volcanol. **29**, 195–222 (1966)
Kuno, H.: Origin of andesite and its bearing on the island-arc structure. Bull. Volcanol. **32**, 141–176 (1968)
Kushiro, I.: Origin of some magmas in oceanic and circum-oceanic regions. Tectonophysics **17**, 211–222 (1975)
Lewis, J.F.: Petrology of the ejected plutonic blocks of the Soufriere Volcano, St. Vincent, West Indies. J. Petrol. **14**, 81–112 (1973)
Macdougall, D.: Particle track records in natural solids from oceans on earth and moon. Ph.D. thesis, Univ. Calif. San Diego, U.S.A. (1972)
Marsh, B.D., Carmichael, I.S.E.: Benioff zone magmatism. J. Geophys. Res. **79**, 1196–1206 (1974)
Meijer, A.: A study of the geochemistry of the Mariana Island Arc system and its bearing on the genesis and evolution of vocanic arc magmas. Ph.D. thesis, Univ. Calif. Santa Barbara, U.S.A. (1974)
Meijer, A.: Pb and Sr isotopic data on the origin of volcanic rocks from the Mariana Island Arc system. Geol. Soc. Am. Bull. **87**, 1358–1369 (1976)
Miyashiro, A.: Volcanic rock series in island arcs and active continental margins. Am. J. Sci. **274**, 321–355 (1974)
Nicholls, I.A.: Petrology of Santorini Volcano, Cyclades, Greece. J. Petrol. **12**, 67–119 (1971)
Nishimori, R.K.: The petrology and geochemistry of gabbroes from the Peninsular Ranges Batholith, California, and a model for their origin. Ph.D. thesis, Univ. Calif. San Diego, U.S.A. (1976)
Peacock, M.A.: Classification of the igneous rock series. J. Geol. **39**, 54–67 (1931)
Philpotts, J.A., Martin, W., Schnetzler, C.C.: Geochemical aspects of some Japanese lavas. Earth Planet. Sci. Lett. **12**, 89–96 (1971)
Pushkar, P.: Strontium isotopes in volcanic rocks of three island arc areas. J. Geophys. Res. **73**, 2701–2714 (1968)
Rea, W.J.: The volcanic geology and petrology of Montserrat, West Indies. J. Geol. Soc. London **130**, 341–366 (1974)
Schmidt, R.G.: Petrology of the volcanic rocks. In: Geology of Saipan, Mariana Islands. U.S.G.S. Prof. Pap. **280** B, 127–175 (1957)
Shapiro, L., Brannock, W.W.: Rapid analysis of silicate rocks. U.S.G.S. Bull. **1036**-C, 19–56 (1956)
Simkin, T., Smith, J.V.: Minor element distribution in olivine. J. Geol. **78**, 304–325 (1970)
Stern, R.J.: Agrigan: An introduction to the geology of an active volcano in the northern Mariana Island Arc. Bull. Volcanol. **41**, 1–13 (1978)
Subbarao, K.V., Hedge, C.E.: K, Rb, Sr and $^{87}Sr/^{86}Sr$ in rocks from the Mid-Indian Oceanic Ridge. Earth Planet. Sci. Lett. **18**, 223–228 (1975)
Taylor, S.R., Kaye, M., White, A.J.R., Duncan, A.R., Ewart, A.: Genetic significance of Co, Cr, Ni, Sc and V content of andesites. Geochim. Cosmochim. Acta **33**, 275–286 (1969)
Wager, L.R.: Igneous cumulates from the 1902 eruption of Soufrière, St. Vincent. Bull. Volcanol. **24**, 93–99 (1962)
Wager, L.R., Brown, G.M.: Layered Igneous Rocks. San Francisco: W.H. Freeman and Co. (1967)
Wright, T.L., Doherty, P.C.: A linear programming and least squares computer method for solving petrologic mixing problems. Geol. Soc. Am. Bull. **81**, 1995–2008 (1970)
Yoder, H.S.Jr.: Calc-alkaline andesites: Experimental data bearing on the origin of their assumed characteristics. In: Proc. of the Andesite Conference (A.R. McBirney, ed.), Oregon Dept. of Geology and Mineral Industries Bull. **65**, 77–89 (1969)
Yoder, H.S., Jr., Tilley, C.E.: Origin of basalt magma: an experimental study of natural and synthetic rock systems. J. Petrol. **3**, 342–532 (1962)

Received May 16, 1978/Accepted November 7, 1978